Neuronal loss, demyelination and volume change in the multiple sclerosis neocortex

Carassiti, D; Altmann, D R; Petrova, N; Pakkenberg, B; Scaravilli, F; Schmierer, K

Published in:
Neuropathology and Applied Neurobiology

DOI:
10.1111/nan.12405

Publication date:
2018

Document version
Publisher's PDF, also known as Version of record

Neuropathology and Applied Neurobiology (2018), **44**, 377–390 doi: 10.1111/nan.12405

Neuronal loss, demyelination and volume change in the multiple sclerosis neocortex

D. Carassiti* , D. R. Altmann†, N. Petrova*, B. Pakkenberg‡, F. Scaravilli* and K. Schmierer*,§

**Blizard Institute (Neuroscience), Queen Mary University of London, †Department of Medical Statistics, London School of Hygiene and Tropical Medicine, London, UK, ‡Research Laboratory for Stereology and Neuroscience, Bispebjerg University Hospital, Copenhagen, Denmark and §Neurosciences Clinical Academic Group, The Royal London Hospital, Barts Health NHS Trust, London, UK*

D. Carassiti, D. R. Altmann, N. Petrova, B. Pakkenberg, F. Scaravilli and K. Schmierer (2018) *Neuropathology and Applied Neurobiology* **44**, 377–390
Neuronal loss, demyelination and volume change in the multiple sclerosis neocortex

Aims: Indices of brain volume [grey matter, white matter (WM), lesions] are being used as outcomes in clinical trials of patients with multiple sclerosis (MS). We investigated the relationship between cortical volume, the number of neocortical neurons estimated using stereology and demyelination. **Methods**: Nine MS and seven control hemispheres were dissected into coronal slices. On sections stained for Giemsa, the cortex was outlined and optical disectors applied using systematic uniform random sampling. Neurons were counted using an oil immersion objective (× 60) following stereological principles. Grey and WM demyelination was outlined on myelin basic protein immunostained sections, and expressed as percentages of cortex and WM respectively. **Results**: In MS, the mean number of neurons was 14.9 ± 1.9 billion *vs.* 24.4 ± 2.4 billion in controls ($P < 0.011$), a 39% difference. The density of neurons was smaller by 28% ($P < 0.001$) and cortical volume by 26% ($P = 0.1$). Strong association was detected between number of neurons and cortical volume ($P < 0.0001$). Demyelination affected 40 ± 13% of the MS neocortex and 9 ± 12% of the WM, however, neither correlated with neuronal loss. Only weak association was detected between number of neurons and WM volume. **Conclusion**: Neocortical neuronal loss in MS is massive and strongly predicted by cortical volume. Cortical volume decline detected *in vivo* may be similarly indicative of neuronal loss. Lack of association between neuronal density and demyelination suggests these features are partially independent, at least in chronic MS.

Keywords: cortical pathology, neuronal loss, progressive multiple sclerosis

Introduction

Multiple sclerosis (MS) is a chronic inflammatory and degenerative disease of the central nervous system (CNS) usually becoming symptomatic in early adulthood [1,2]. The most obvious pathological findings in the MS brain consist of focal white matter (WM) demyelination with microscopic analysis further revealing perivascular and parenchymal inflammation, a variable degree of axonal loss, remyelination and gliosis [3].

Although involvement of the grey matter (GM) in MS pathology has been described for well over one century [4–9], the past two decades have seen an increased interest in measuring the extent, and identifying the cellular basis, of cortical pathology in people with MS (pwMS), notably demyelination and neuronal loss [10–13].

Magnetic resonance imaging (MRI) studies assessing various indices of cortical damage suggest that clinical measures of disability may be more closely related to

Correspondence: Klaus Schmierer, Blizard Institute (Neuroscience), 4 Newark Street, London, E1 2AT, UK. Tel: +44 20 7882 6246; Fax: +44 20 7882 2180; E-mail: k.schmierer@qmul.ac.uk

GM than WM pathology, particularly after onset of progression [14–17].

However, the histological correlate(s) of volume changes across the whole neocortex have not been systematically assessed. Given that indices of brain volume have emerged as key outcome measures in natural history studies and treatment trials of new disease modifying agents, establishing the quantitative cellular basis of volumetric changes in the brain is of significant importance [18].

Although previous observations have established the presence of neuronal loss in the MS neocortex, there is significant variation in the reported magnitude, ranging between 18% [19] and up to 65% in individual cortical layers [13]. The variation in the degree of neuronal loss reported in these studies may have arisen from variability in the available *post mortem* material, differences in sampling strategy and the application of a two-dimensional approach to histological quantification [20].

Moreover, the impact of neocortical demyelination on neuronal loss and cortical volume across the whole brain has remained unclear. Peterson and co-workers described an increase of neuronal apoptosis in demyelinated neocortex [21]; however, the reported association between neuronal loss and demyelination was either mild (10% loss in demyelinated *vs.* nondemyelinated cortical areas) or nonsignificant [13,19,22,23]. Given the difficulties detecting cortical lesions using MRI *in vivo* as well as *post mortem*, at least when using standard clinical MR systems [24–26], careful quantitative autopsy studies to further explore the association between myelination status, neuronal loss and cortical volume change are warranted [27].

In this study, we quantified the number of neurons across the whole neocortex of pwMS using unbiased stereological methods to estimate the overall extent of neuronal loss. We then investigated the association between the number of neocortical neurons and (i) the degree of cortical and WM demyelination and (ii) cortical and WM volume.

Materials and methods

Brain specimens and clinical data

This study was performed on formalin-fixed *post mortem* brain hemispheres from nine pwMS, seven secondary progressive (SP) MS and two primary progressive (PP) MS, of which six were female and three male. Control brain tissues from seven healthy donors (three females and four males) with no history or pathological evidence of neurological disease were used as a reference. MS cases were selected to provide a wide age range at death (Table 1).

The diagnosis of MS, as well as the absence of any other confounding pathology in our cohort of cases, was confirmed based on the patient history (reviewed by Klaus Schmierer and Daniele Carassiti) and on a detailed neuropathological inspection (conducted by Francesco Scaravilli, Daniele Carassiti, Natalia Petrova and Klaus Schmierer): at least five tissue blocks, dissected without compromising the integrity of the neocortex for subsequent stereological analysis, were sampled from the following regions: hippocampus and entorhinal cortex, F2 frontal cortex, the pericallosal gyrus, corpus callosum and the periventicular WM, occipital and temporal cortices. We then assessed with light microscopy the presence of inflammatory infiltrates and described the demyelinated lesions according to Kuhlmann and colleagues [28]. All dissected tissue blocks were stained for haematoxilin and eosin, Luxol fast blue and immunostained for CD68 to reveal microglial cells. In 7 out of 16 cases with an older age at death (two controls and five MS, aged 92 and 81 and 55–73 years respectively), immunohistochemistry (IHC) was carried out to assess the presence of Lewy bodies, β-amyloid and neurofibrillary (NFT) tangles. The antibodies used and corresponding immunohistochemical methods are summarized in Table S1.

Tissue dissection

Following the separation of the cerebellum and brainstem from the forebrain at the level of the midbrain, the hemispheres were separated by an anteroposterior cut through the corpus callosum and weighed. Lobar topography was marked on the cortical surface using tissue dye (Sigma-Aldrich, St. Louis, Missouri, USA) so that the three frontal gyri, the motor, the parietal/temporal and the occipital cortices, were identified. Brain hemispheres were then dissected into parallel coronal slices with a thickness of 11 mm using a custom-made Perspex tissue holder including cutting panel (Schmierer GmbH, Gross-Gerau, Germany). The total surface area of each formalin-fixed coronal slice was measured before and after

Table 1. Clinical information on all *post mortem* MS and control specimens included in this study

MS case/subtype *Cause of death*	*Sex*	*Age at onset*	*Age at wheelchair*	*Age at death*	*PMD (h)*	*Fixation time (m)*	*Hemisphere weight (g)*
MS 232/SP Bronchopneumonia	M	40	72	92	23	129	472
MS 453/SP Pneumonia	M	28	48	68	33	58	514
MS 455/PP Chest infection	F	50	55	69	32	59	463
MS 463/SP Bronchopneumonia	F	17	27	47	39	55	412
MS 464/PP Bronchopneumonia	F	57	n.d.	61	41	43	535
MS 468/SP Unknown	F	24	n.d.	55	48	45	555
MS 471/SP Pulmonary fibrosis, asbestos exposure	F	60	86	86	47	53	456
MS475/PP Pneumonia (bilateral)	M	58	67	73	12	52	448
MS 550/SP Urinary infection	F	42	59	64	n.d.	36	442

Case	*Sex*	*Age at death*	*PMD*	*Fixation time (m)*	*Hemisphere weight (g)*	*Cause of death*
C50	F	53	12	336	573	Myocardial infarction
C55	F	92	60	336	498	Cardiac arrest
C56	M	82	50	58	490	Aspiration pneumonia
C58	M	89	15	50	485	General deterioration
C60	M	78	10	47	525	Pancreatic cancer
C61	M	81	27	47	669	Ischaemic heart disease
C188	F	47	24	324	625	Metastatic ovary cancer

PMD, *post mortem* delay; h, hours; m, months; g, grams; M, males; F, females; MS, multiple sclerosis; SP, secondary progressive; PP, primary progressive.

tissue processing. The tissue shrinkage factor (SF) was then calculated and expressed as a percentage loss of the formalin-fixed surface area prior to tissue processing.

Tissue processing, embedding and staining

Coronal slices were processed for paraffin-embedding using a Thermo Scientific Excelsior ES tissue processing machine (Kalamazoo, Michigan, USA). Due to the thickness of the brain slices the processing protocol was optimized to a duration of 80 h. All samples were first immersed in industrial methylated spirit at 30°C for 39 h (divided into six steps of 1, 4, 6, 8, 10 and 10 h), then dehydrated in toluene at 30°C for 14 h (three steps of 4, 5 and 5 h), followed by a final incubation in liquid paraffin at 62°C for 27 h (three steps of 6, 9 and 12 h). For each incubation step the solution was automatically changed and stirred. During embedding each slice was kept in the same orientation as it had been during dissection. Care was taken to embed the cutting side parallel to the surface of the paraffin block. Whole hemispheric sections were then cut using a Reichert-Jung Tetrander. The first 40-µm-thick section including the entire hemispheric surface of the coronal slice was mounted on precoated glass slides and instantly dried at 40°C for 24 h, then preheated at 60°C for at least 2 h before dewaxing in xylene, rehydrating in industrial methylated spirit and staining with modified Giemsa stain solution (50 ml Giemsa by Merck, Kenilworth, NJ, USA cat. no. 1.09204, with 200 ml potassium–hydrogen–phosphate at pH 4.5 for 1 l of final solution, filtered before use) for about 3 h. Finally the sections were differentiated with 0.5% acetic acid and dehydrated before mounting them in DPX mounting medium (VWR, Radnor, PA, USA).

Stereological analysis

Stereological analysis (DC) was performed using a stereology workstation consisting of a modified light microscope (Nikon Eclipse 80i, Minato, Tokyo, Japan) equipped with a PlanUW objective 2× [numerical aperture (NA) = 0.06], a 60× PlanApo oil-immersion objective (NA = 1.4) (Nikon, Tokyo, Japan), an integrated motorized stage for automated sampling (MBF Bioscience, Williston, VT, USA), a CCD colour video camera (CX9000; MBF Bioscience) and stereology software (StereoInvestigator; MicroBrightField, Williston, VT, USA).

Forty-μm-thick Giemsa-stained coronal hemispheric sections were inserted on a custom-made section holder, and then area of interest (AOI), in this case the whole neocortical ribbon, was manually outlined and measured using a 2× objective. The neocortical volume was calculated for each slice using the following equation:

$$V_{\text{slice}} = \text{AOI} \times T, \quad (1)$$

where T was the distance between sections [29]. The total number of neurons per slice was equal to the volume of the reference space (neocortex) per slice multiplied by the numerical density of neurons = N_V. The N_V was equal to the total number of neurons counted in the slice ($\sum$Q-) divided by the total volume of all disectors in which those neurons were sampled = $\sum$Q-/$\sum$disectors volume. The volume of one disector was equal to the area of the frame of the disector, 50 × 50 μm, multiplied by the height of the disector (20 μm), that is, 50 000 μm^3. StereoInvestigator Software placed disectors over the AOI using a systematic uniform random sampling protocol and an x–y step length of x = 3455 μm and y = 4655 μm. Step lengths were defined such that even the smaller AOIs, for example, in the most anterior slices of the frontal cortex and the most posterior ones in the occipital cortex, would be covered by at least 10 disectors and were then kept constant for all samples. The protocol thereby avoided underestimation of these cortical regions. The cell counting was performed using the optical disector method [30–32]. The method is a slight modification of existing techniques, which have been considered efficient and reliable in studies of rat [33] and human neocortex [34]. The optical disector is a three-dimensional probe generated with the aid of a microscope with a high numerical aperture and oil immersion objective, in which it is possible to observe thin focal planes in relatively thick sections. A counting frame with 'exclusion' and 'inclusion' lines was superimposed on the magnified image of the tissue on a computer screen and the orientation in the z-axis was measured with a digital microcator with a precision of 0.5 μm. The purpose of 'exclusion' and 'inclusion' lines of the counting frame is to exclude edge effects arising from subsampling [35]. All cells that come into focus within the frame and not in focus at the uppermost position were counted as the focal plane was moved 20 μm through the section. Giemsa-stained neurons were identified according to the following morphological criteria: a triangular cellular shape, a vesicular nucleus, a single large nucleolus free of any surrounding heterochromatin and a visible cytoplasm with interspersed ribosomes [36]. The neuronal nucleus was used as the counting item: on average, 125 ± 54 neuronal nuclei were counted per slice, with an average number of neurons of 1787 ± 522 counted for each brain (mean ± SD). The number of neurons in each slice was subsequently calculated according to:

$$N_V \times V_{\text{ref}} \quad (2)$$

and the total number of neocortical neurons (TNNN) determined as the sum total number of neurons in all slices from one hemisphere multiplied by two (Figure 1**A**–**C**). This result is an unbiased estimate as the hemispheres were chosen systematically at random based on the assumption that both brain hemispheres in one individual contain the same number of neocortical neurons (in control cases: 4 right *vs.* 3 left hemispheres; in MS cases: 2 right *vs.* 7 left; in the whole cohort: 5 right *vs.* 11 left).

To explore association between TNNN and WM volume, the latter was also manually outlined and calculated as described above for cortical volume.

Quantification of demyelination

The extent of GM and WM demyelination was manually outlined on 10-μm-thick hemispheric coronal sections, adjacent to Giemsa-stained sections (Figure 2**A**), using myelin basic protein (MBP) IHC (SMI-94; Covance, Cambridge Bioscience, London UK) following an established protocol [26] (Figure 2**B**). The

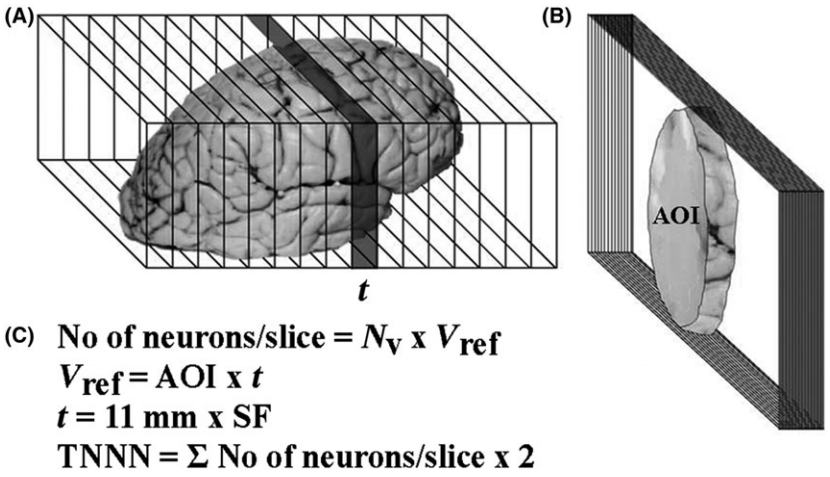

Figure 1. Stereology. Indices acquired for unbiased estimates of the total number of neocortical neurons (TNNN). Each brain hemisphere was dissected into parallel coronal slices (**A**). The neocortical area of interest (AOI) was then manually outlined and measured (**B**). The AOI was then multiplied by the slice thickness (t), which was adjusted by the shrinkage factor (SF), to obtain the cortical volume estimate of that slice (V_{ref}). This volume was then multiplied by the density of neurons counted in the disectors placed within that slice (N_v). TNNN was then obtained as the sum total of neurons in each slice multiplied by 2 (**C**). Adapted from Artacho-Pérula *et al.* 2004, Brain Res [37].

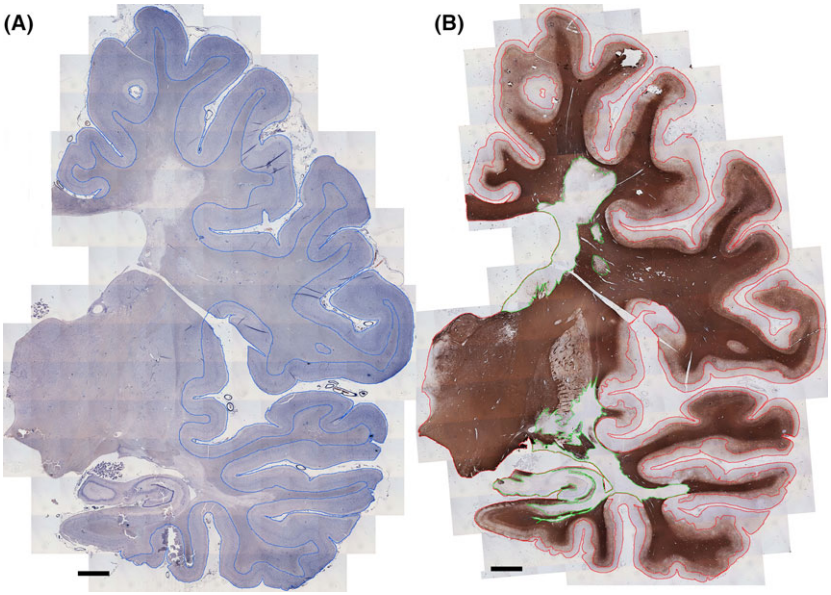

Figure 2. Assessment of cortical volume and demyelination. Exemplary adjacent sections of a hemispheric coronal multiple sclerosis brain slice stained for Giemsa (**A**) and immunostained for myelin basic protein (**B**). The blue line indicates the border between white matter (WM) and neocortex, the red and green lines indicate cortical and WM demyelination respectively. Images acquired with a × 2 objective. Scale bars = 1 cm.

quantification of demyelination was performed on a mean of 6 (range = 4–14) slices/hemisphere selected using systematic uniform random sampling covering all cortical regions investigated.

All images were acquired at × 2 magnification using the stereology workstation with optimized settings for light intensity, exposure and white balance, depending on the objective in use and kept constant during every acquisition session. Images were saved as .TIFF files with spatial reference information settings for each objective based on calibration images.

Files were then opened using ImageJ Software Developed by Wayne Rasband (retired from NIH) as public domain software, and GM demyelination manually outlined on the digitized images of MBP immunostained sections, including all cortical lesion types [21], and expressed as a percentage of the total cortex on each slide. The same images were used to manually outline WM demyelination.

Statistical analysis

Demographics are reported as mean ± SD and compared using Student's *t*-test. Differences between pwMS and controls were examined using linear mixed models with the measure being compared as the response variable, and a fixed effect group indicator; fixed effect cortical region indicators were included in all models, and other potential confounders (age, gender, SF and disease duration, for which controls were assigned a zero value in comparisons with pwMS) were included singly as fixed effect covariates. These models used the coronal slice as the unit of analysis, with a random subject intercept to account for the ownership of slices by subjects. Possible variations in pwMS *vs.* control differences by region were examined by adding a group × region interaction term to the models. Linear mixed models were also used to investigate associations, in patients only, between cortical pathology measures. Residuals were examined to check model assumptions, as a result of which number of neurons, cortical and WM volumes per slice were log transformed, which generally improved residual normality and homoscedasticity. Restricted maximum likelihood estimation was used except where there was evidence of residual heteroscedasticity, when maximum likelihood was used with robust standard errors. Pearson's test was used only to investigate the association between the entire cortical volume and the total number of neurons with a whole brain as a unit of analysis. All calculations were performed in Stata 13 (Stata Corporation, College Station, TX, USA) and Prism 6 (GraphPad, San Diego, CA, USA) and significance is reported at 5%.

Results

Histological sampling and cohort details

A total of 16 cerebral hemispheres were dissected into 229 coronal slices (14 slices/hemisphere, range = 13–17 slices) and analysed in this study. pwMS did not differ from controls with respect to age at death (68 ± 14 years, range = 47–92 years *vs.* 75 ± 18 years, range = 47–92, $P = 0.44$), *post mortem* delay (34 ± 12 h *vs.* 29 ± 19 h, $P = 0.5$) and fixation time (59 ± 27 months *vs.* 171 ± 150 months, $P = 0.26$), the latter was in particular very long for three female controls, however, these outlier data does not affect our analysis and overall observations. Hemispheres of pwMS were lighter than controls (477 ± 47 g *vs.* 552 ± 72 g, $P = 0.02$), a 14% difference, and SF after processing more pronounced in pwMS than in controls (28 ± 11% and 25 ± 11%, *t*-test $P = 0.027$).

Microscopic inspection of tissue blocks for pathology reporting showed only sparse inflammation, either in WM parenchyma or within perivascular spaces or in the depth between two banks of a gyrus, where meningeal inflammation has been reported to be found more frequently [11]. Therefore, we did not characterize meningeal inflammation any further in our cohort. No active WM lesions were observed.

In order to rule out possible comorbidity, such as Parkinson's or Alzheimer's disease, we investigated sections using morphological and IHC methods. No evidence of Lewy bodies or α-synuclein-positive intracytoplasmatic inclusions was found in any of the brains examined (Figure S1**D**,**G**). A β-amyloid deposition was also absent from the hippocampus of all controls and MS cases (not shown). In one MS case

Figure 3. Neocortical neuronal numbers and their correlation with tissue volumes and demyelination in nine multiple sclerosis brain hemispheres and seven controls. The total number of cortical neurons in men (dots) and women (squares) with multiple sclerosis (MS) was 39% lower compared to control brains (**A**) while the density of neurons was lower by 28% (**B**). The mean proportion of tissue demyelinated was fourfold greater in the grey compared to the white matter (**C**). No statistically significant evidence was detected for an association between neuronal density and cortical grey matter demyelination (**D**). However, strong correlation was detected between the number (*n*) of cortical neurons and cortical volume in MS (**E**) and controls (**F**). This association was also confirmed using Pearson's correlation (**G**). Weak correlation was detected between white matter volume and *n* cortical neurons (**H**). In **A**, **B** and **G** values are presented using 'whole brain' as the unit of analysis; **C**–**F**, **H** are presented on a 'per brain slice' basis. Error bars and dotted lines represent 95% confidence intervals.

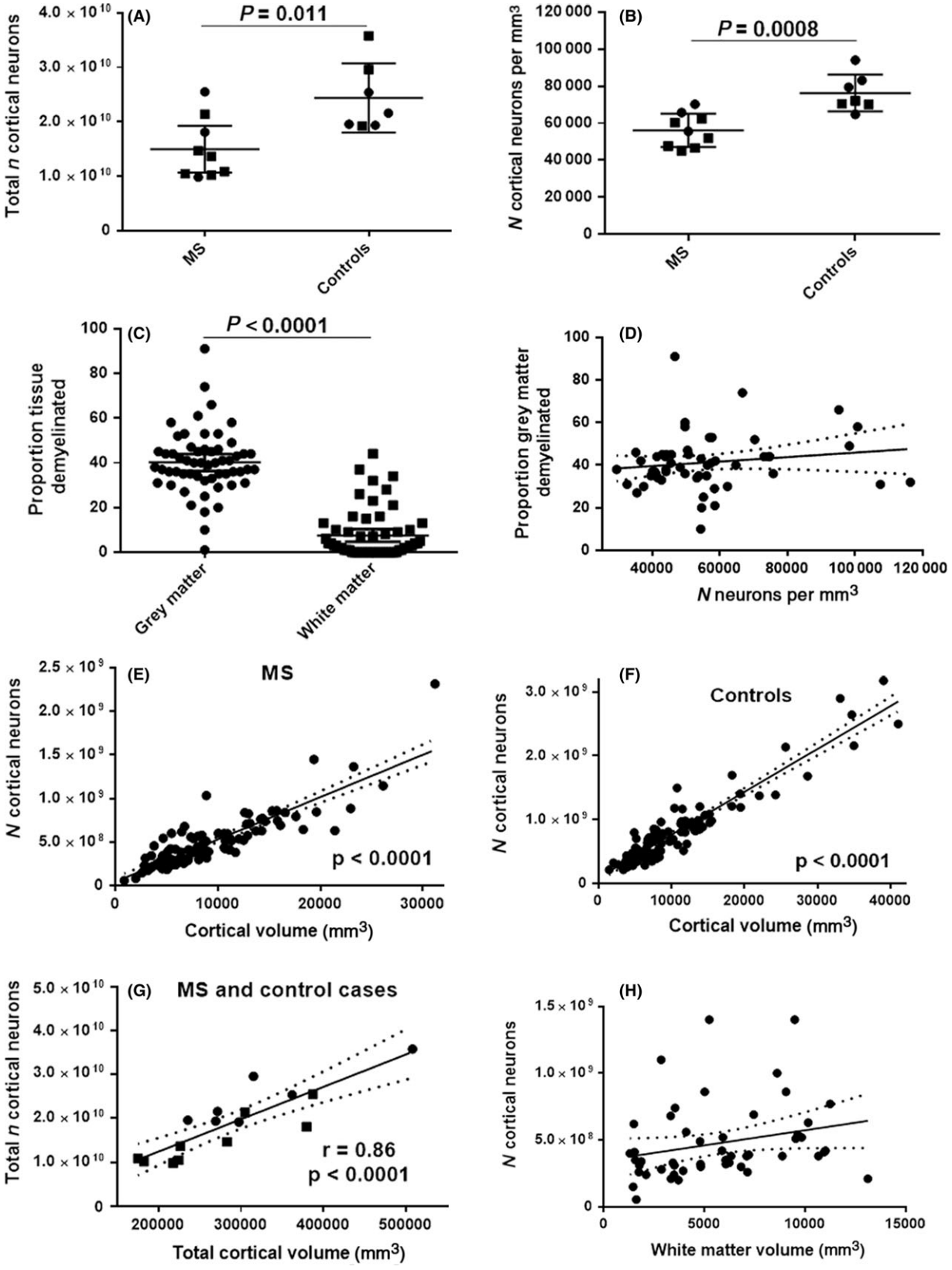

(MS455), diffuse αβ-amyloid plaques in the neocortex were observed; a few such plaques were also seen in the neocortex of the oldest control case (C55) (Figure S1**E**,**H**). The same control (92-year-old) was also found to have very sparse NFT-positive neurons in the dentate gyrus, and also some in the neocortex (Figure S1**F**). Similarly, a very low numbers of NFT-positive neocortical neurons were observed in two MS patients (MS475 and MS455, Figure S1**I**).

Loss of neocortical neurons in MS

In pwMS, the TNNN was 14.9 ± 1.9 billion *vs.* 24.4 ± 2.4 billion in controls (mean ± SD) showing that there were 39% fewer neurons in the neocortex of pwMS than in controls after adjusting for age, gender, disease duration and SF [95% CI (13, 58), $P = 0.011$, Figure 3**A**). There was no evidence that this difference varied significantly across the frontal, motor, parietal/temporal and occipital cortical regions ($P = 0.72$). The number of neurons in each cortical region are listed in Table 2.

Extent of neocortical 'atrophy' in MS

After adjustment for age, gender, disease duration and SF, we detected trend difference in total cortical volume with pwMS having a 26% smaller cortical volume than controls ($P = 0.1$). There was no evidence of different volume reductions across the four cortical regions analysed ($P = 0.77$).

Lower neuronal density in the MS neocortex

After adjusting for age, gender, disease duration, cortical region and SF, the mean neuronal density [neurons/mm^3 ± SEM] in pwMS was 57 468 ± 3636 and 79 787 ± 3869 in controls (mean ± SEM, $P = 0.0008$) indicating a significant 28% reduction in neuronal density (Figure 3**B**). Neuronal density was significantly smaller in women compared to men, in pwMS ($P < 0.001$) and in controls group ($P < 0.001$). See Table 3 for the mean neuronal density and the proportional decrease in neuronal density measures in pwMS and controls, both males and females.

We observed a significant decrease of neuronal density in each cortical region in pwMS when compared to controls (see Table 4, all *P*s < 0.001).

As expected, we detected a significantly higher neuronal density in the occipital cortex compared to the other cortical regions in both MS and controls ($P < 0.001$). There was no statistical evidence that the difference in the neuronal density observed between cortical regions followed a different pattern in pwMS and controls ($P = 0.615$).

The extent of demyelination

The degree of demyelination was quantified in 57 hemispheric coronal sections of nine MS cases. The nonadjusted mean proportion of demyelinated cortex in

Table 2. Total number of neurons in each cortical region of one brain hemisphere in people with MS and in controls expressed as mean ± SD

Cortical region	*MS (× 10^9)*	*Controls (× 10^9)*
Frontal	1.75 ± 0.93	3.08 ± 1.4
Motor	1.39 ± 0.78	3.25 ± 0.91
Parietal/temporal	2.6 ± 1.3	3.4 ± 1.1
Occipital	1.8 ± 0.77	2.5 ± 1.5

MS, multiple sclerosis.

Table 3. Average neuronal densities and relative loss of neocortical neurons comparing female and male, people with MS and controls

	Males	*Females*	*Difference (%)*
MS brain	67 051 ± 5716	54 236 ± 3922	12 815 (19)
Control brain	84 185 ± 4597	73 649 ± 5153	10 536 (12)
Loss (%)	17 134 (20)	19 413 (26)	

Mean ± SEM (neurons/mm^3).
MS, multiple sclerosis.

Table 4. Average neuronal densities and the relative loss of neocortical neurons comparing frontal, motor, parietal/temporal and occipital cortices of people with MS with controls

Cortical region	*Patients*	*Controls*	*Difference (%)*
Frontal	51 060 ± 4002	73 163 ± 4219	22 103 (30)
Motor cortex	54 145 ± 4213	77 520 ± 4402	23 375 (30)
Parietal/ temporal	52 859 ± 4191	76 450 ± 4431	23 591 (30)
Occipital	73 773 ± 4199	96 863 ± 4440	23 090 (24)

Mean ± SEM (neurons/mm^3).

Table 5. Average proportion of demyelinated grey matter (mean ± SEM) affecting the four cortical regions analysed showing that lesion load is significantly affecting the frontal cortex more than motor, parietal/temporal and occipital cortices

Cortical region	*Demyelinated cortex % ± SEM*
Frontal	46 ± 6
Motor cortex	38 ± 6
Parietal/temporal	39 ± 7
Occipital	33 ± 6

MS was 40 ± 13%. There was no evidence that demyelination varied by gender ($P = 0.99$), age ($P = 0.794$) or disease duration ($P = 0.2$). All cortical regions included in our analysis showed significantly less demyelination than frontal cortex (motor cortex, $P = 0.004$; parietal and temporal cortices, $P = 0.017$; occipital cortex $P < 0.001$) which was the most severely affected (see Table 5 for the relative demyelination in each cortical region).

There was no significant gender difference in terms of proportional cortical demyelination between males and females (M = 42 ± 11%, F = 39 ± 7%; $P = 0.737$).

The mean proportion of demyelination in WM (9 ± 12%) was fourfold smaller than in the GM ($P < 0.0001$, Figure 3**C**). There was no evidence that WM demyelination varied by gender ($P = 0.43$), age ($P = 0.11$) or disease duration ($P = 0.99$).

No association between neuronal loss and demyelination

After adjusting for age, gender and SF, no significant association was detected between the percentage of cortical demyelination and the neuronal density, neither across the entire cortex ($P = 0.21$, Figure 3**D**) nor in specific cortical regions ($P = 0.322$). No association was detected either between the number of cortical neurons and WM lesion volume ($P = 0.11$).

Association between number of cortical neurons and tissue volumes

After adjusting for age, gender and SF, a greater cortical volume correlated strongly with a greater number of cortical neurons ($P < 0.001$). This correlation, when tested in each brain slice, was significantly different in pwMS compared to controls ($P < 0.001$), with pwMS showing a shallower regression line (49 787/mm^3) than controls (68 848/mm^3), thereby indicating lower neuronal density in the MS cortex (Figure 3**E**,**F**). In addition, we detected significant correlation between WM volume and the number of neocortical neurons in the same slab: for each additional mm^3 of WM volume, we detected a corresponding increase of 0.005% in the number of neocortical neurons ($P = 0.004$, Figure 3**H**). Further statistical calculations, applying instead the Pearson's test on the 'total cortical volume' and the 'total n cortical neurons' as the unit of analysis, confirmed a strong association between these two quantities (Figure 3**G**, $r = 0.86$; $P < 0.0001$).

Discussion

Given various *in vivo* indices of brain volume are in use to monitor treatment effect in clinical trials of pwMS, it is important to accurately establish the histological correlates of brain volume changes [38,39]. In this study, we focussed on the MS neocortex using an unbiased histological sampling technique and applied the rules of stereology in order to accurately quantify in *post mortem* brain the extent of neuronal loss across the entire neocortex in pwMS and controls and the correlation between the number of neurons, cortical volume and cortical demyelination.

After a mean disease duration of 27 years, pwMS had 39% lower TNNN compared to controls highlighting the substantial loss of the key CNS cell type – neurons – during a life with MS. Neuronal density was reduced by just under 30%, and as with neuronal loss, this decrease was a global finding, that is, there was no difference in terms of proportional neuronal loss among the lobes investigated, including the occipital (visual) cortex which – in line with its specific anatomical organization of layers – showed a higher density of neurons compared to the frontal, motor, parietal and temporal cortices. The detected reduction of TNNN in MS, over and above the reported 10% due to ageing [34], underlines the significance of neuronal loss in the MS neocortex. Negligible signs of additional pathology in a few of our cases are unlikely to have affected the stereological estimates in our study.

While the difference in cortical volume between MS and controls did not reach statistical significance, the number of neocortical neurons was robustly associated

with the cortical volume in both MS brain and control tissue (Figure 3**E**–**G**). There are, of course, some caveats in comparing results derived from histology of processed *post mortem* tissue with data acquired using MRI in pwMS *in vivo*. The process of fixation leads to changes of MRI indices, such as relaxation times and diffusion [40,41]; some degree of shrinkage may have taken place as a result of tissue fixation [42], over and above the volume reduction due to the dehydrating process of tissue embedding, which in our sample was 25–28%.

In spite of the above-mentioned limitations, we therefore infer from the association between the number of cortical neurons and the cortical volume detected in our study that indices of cortical volume acquired using MRI may provide a reasonable estimate of the number of neocortical neurons during life. The weak association between WM volume and the number of neocortical neurons in pwMS underpins *in vivo* MRI studies indicating WM volume is a far less robust predictor of cortical pathology [43,44].

While the difference in total cortical volume between MS and controls did not reach statistical significance, the magnitude of this difference – 26% smaller volume in MS brain – would be consistent with an annual cortical atrophy of just under 1%, which is similar to figures obtained using MRI in pwMS *in vivo* [44].

Several MRI studies reported regional variation of cortical volume reduction in pwMS [45,46]. However, we did not detect such variation with the degree of cortical volume loss being very similar across all regions. One explanation for this difference would be that local volume variation may present at early disease stages and becomes less apparent in chronic MS [47,48].

Significant neocortical demyelination was detected in our samples. The degree of demyelination varied, similar to previous observations [11], between 46% (frontal cortex) and 33% (occipital cortex), which is in contrast to our cortical volume measures that suggested a virtually identical degree of atrophy across all lobes. While earlier pathology studies suggested a mild effect (10%) of cortical demyelination on neocortical neuronal loss [13,21,22], our study did not reveal any association whatsoever between the extent of demyelination and the density of neurons in the MS neocortex. This finding corroborates recent research on a smaller number of tissue samples which indicated neuronal loss in the MS neocortex compared to controls, however, showing no difference in the number of neurons between lesional and nonlesional MS neocortex [23].

The observed lack of association between the volume of WM and both the neocortical myelination and neuronal loss in each slab, suggests that, at least in advanced stages of MS, these two key pathological features may become partially independent. Assuming an association between demyelination and neuroaxonal loss does exist in early MS, well described for acute lesions in the WM [49,50], the detected lack of such relationship in the GM in late stage MS remains poorly understood. Numerous hypotheses are being explored including the contribution of anterograde (Wallerian) and retrograde ('dying back') axonal degeneration [51] due to remote lesions located some distance away [52,53], meningeal inflammation [11] not necessarily targeting myelin proteins [54], chronic microglia activation [55], gliosis [56], oxidative stress and mitochondrial dysfunction [57], primary neurodegenerative processes [58] and exhaustion of CNS repair mechanisms [59], all of which may contribute to worsening disease in pwMS without overt inflammatory demyelination [12].

While lesions detected using conventional T_2-weighted MRI in patients with long-standing MS are not specific for the underlying tissue condition (de-/remyelination, axonal damage, gliosis, inflammation, etc.), the majority of those lesions will be of the chronic inactive type with significant axonal loss and sparse remyelination [60]. And while chronic disease deterioration is rather uniform and relentless [61], association with lesions on T_2-weighted MRI as a proxy of inflammatory demyelination is no longer robust at this stage, in line with the relative independence of disability accrual (considered driven by neuroaxonal loss) from relapses (considered the clinical manifestation of inflammatory demyelination) [62]. These findings are also corroborated by the poor response of people with worsening MS to purely systemic immunomodulatory and immunosuppressive therapy [63]. The poor prediction of disability based on lesions detected on T_2-weighted MRI is one of the key reasons why measures of brain volume have become such important indices to predict clinical outcome.

The lack of correlation in chronic MS between neocortical demyelination and neuronal loss is also strikingly similar to the lack of such association between the total amount of demyelination and axonal loss in

the chronic MS spinal cord [64]. It will be of interest to investigate these relationships using *post mortem* tissue of the entire neuraxis, which to our knowledge has only been performed once in a relatively limited sample [65].

Limitations of the study

While the observed cortical atrophy could be caused entirely by the loss of neurons, its cellular basis should be addressed in further stereology studies also assessing: neuronal size, dendritic and synaptic pathology and the loss of other neocortical cell populations, such as microglia and oligodendrocytes.

In particular, dysfunction and loss of synapses, a pathological finding common to a number of chronic neurological diseases [66], has recently received attention also in the context of MS and its animal model experimental autoimmune encephalitis [67]. In pwMS, synaptic loss has been reported in the hippocampus associated with demyelination [68] and the presence of the complement system proteins C1q and C3 [69]. Subsequent studies reported synaptic damage and loss in the cortical GM [22,70,71] and the cerebellar dentate nucleus [72]. It is possible that synaptic loss could contribute as an additional factor to cortical atrophy together with the observed neuronal loss. Further studies are therefore warranted to investigate the interrelationship between synaptic loss, demyelination and volume change in pwMS.

In spite of these limitations, the strength of the detected association between cortical volume and number of neurons in our data, corroborated by recent evidence from a MRI/pathology study [27], supports the use of MRI indices of brain – particularly cortical – atrophy as a predictor of neuronal loss.

In conclusion, we provide robust evidence that in chronic MS (i) neocortical neuronal loss is ultimately decreased by nearly 40%, (ii) the impact of demyelination on neuronal density as well as cortical volume appears limited and (iii) cortical volume is a strong predictor of number of cortical neurons. By inference, we hypothesize MRI indices of cortical and brain atrophy can provide a useful tool to predict an important degenerative component of MS. Further validation of this hypothesis through correlative MRI/pathology studies is warranted.

Acknowledgements

We thank the UK Multiple Sclerosis Tissue Bank, particularly Richard Reynolds, Djordje Gveric and Sue Fordham for supplying tissue used in this study; Christopher Evagora, Pauline Levey, Rebecca Carrol and Mark Childs (Core Pathology, Blizard Institute at Queen Mary University) for laboratory support; Agniezska Jakubowska for technical support; Maria-Marta Papachatzaki for her help during an earlier stage of this study and Hans Lassmann for his comments on the draft manuscript. KS has been supported by a Higher Education Funding Council for England Clinical Senior Lectureship. This work was supported by Barts Charity (grant code 468/1506). All MS cases and four controls were obtained from the UK Multiple Sclerosis Tissue Bank, which is covered by Research Ethics Committee reference number 08/MRE09/31. Three additional controls were provided by BP and covered by license number: 2007-58-0015/H-C-2009-027.

Author contributions

KS, BP, DC and FS conceived and designed the study. DC, KS, DRA, NP and FS acquired and analysed the data. DC and KS drafted the manuscript and figures.

Conflicts of interest

The authors have no conflicts of interest with regard to the contents of this study.

References

1 Reynolds R, Roncaroli F, Nicholas R, Radotra B, Gveric D, Howell O. The neuropathological basis of clinical progression in multiple sclerosis. *Acta Neuropathol* 2011; **122**: 155–70.
2 Compston A, Coles A. Multiple sclerosis. *Lancet* 2008; **372**: 1502–17
3 Lassmann HW. *McAlpine's Multiple Sclerosis* 4th edn. [Book Chapter]. Amsterdam, Netherlands: Elsevier, 2006.
4 Marburg O. *Die sogenannte akute multiple Sklerose (Encephalomyelitis Periaxialis Scleroticans)*. Leipzig: F. Deuticke, 1906.
5 Brownell B, Hughes JT. The distribution of plaques in the cerebrum in multiple sclerosis. *J Neurol Neurosurg Psychiatry* 1962; **25**: 315–20

6 Sander D. Hirnrindenbefunde bei multipler Sklerose. *Monatsschr Psychiatr Neurol* 1898; **IV**: 29–39.
7 Dinkler M. Zur Kasuistik der multiplen Herdsklerose des Gehirns und Ruckenmarks. *Deuts Zeits Nervenheilik* 1904; **26**: 233–247
8 Schob F. Ein Beitrag zur patologischen Anatomie der multiplen Sklerose. *Monatsschr Psychiatr Neurol* 1907; **22**: 62–87
9 Dawson JD. The histology of multiple sclerosis. *Trans R Soc (Edinb)* 1916; **50**: 517–740
10 Geurts JJ, Barkhof F. Grey matter pathology in multiple sclerosis. *Lancet Neurol* 2008; **7**: 841–51
11 Howell OW, Reeves CA, Nicholas R, Carassiti D, Radotra B, Gentleman SM, Serafini B, Aloisi F, Roncaroli F, Magliozzi R, Reynolds R. Meningeal inflammation is widespread and linked to cortical pathology in multiple sclerosis. *Brain* 2011; **134**(Pt. 9): 2755–71.
12 Lucchinetti CF, Popescu BF, Bunyan RF, Moll NM, Roemer SF, Lassmann H, Bruck W, Parisi JE, Scheithauer BW, Giannini C, Weigand SD, Mandrekar J, Ransohoff RM. Inflammatory cortical demyelination in early multiple sclerosis. *N Engl J Med* 2011; **365**: 2188–97
13 Magliozzi R, Howell OW, Reeves C, Roncaroli F, Nicholas R, Serafini B, Aloisi F, Reynolds R. A Gradient of neuronal loss and meningeal inflammation in multiple sclerosis. *Ann Neurol* 2010; **68**: 477–93
14 Fisniku LK, Brex PA, Altmann DR, Miszkiel KA, Benton CE, Lanyon R, Thompson AJ, Miller DH. Disability and T2 MRI lesions: a 20-year follow-up of patients with relapse onset of multiple sclerosis. *Brain* 2008; **131**(Pt. 3): 808–17.
15 Fisniku LK, Altmann DR, Cercignani M, Tozer DJ, Chard DT, Jackson JS, Miszkiel KA, Schmierer K, Thompson AJ, Miller DH. Magnetization transfer ratio abnormalities reflect clinically relevant grey matter damage in multiple sclerosis. *Mult Scler* 2009; **15**: 668–77
16 Filippi M, Horsfield MA, Tofts PS, Barkhof F, Thompson AJ, Miller DH. Quantitative assessment of MRI lesion load in monitoring the evolution of multiple sclerosis. *Brain* 1995a; **118**(Pt. 6): 1601–12
17 Filippi M, Paty DW, Kappos L, Barkhof F, Compston DA, Thompson AJ, Zhao GJ, Wiles CM, McDonald WI, Miller DH. Correlations between changes in disability and T2-weighted brain MRI activity in multiple sclerosis: a follow-up study. *Neurology* 1995b; **45**: 255–60
18 Sormani MP, Arnold DL, De Stefano N. Treatment effect on brain atrophy correlates with treatment effect on disability in multiple sclerosis. *Ann Neurol* 2014; **75**: 43–9
19 Vercellino M, Plano F, Votta B, Mutani R, Giordana MT, Cavalla P. Grey matter pathology in multiple sclerosis. *J Neuropathol Exp Neurol* 2005; **64**: 1101–7
20 Abercrombie M. Estimation of nuclear population from microtome sections. *Anat Rec* 1946; **94**: 239–47
21 Peterson JW, Bo L, Mork S, Chang A, Trapp BD. Transected neurites, apoptotic neurons, and reduced inflammation in cortical multiple sclerosis lesions. *Ann Neurol* 2001; **50**: 389–400
22 Wegner C, Esiri MM, Chance SA, Palace J, Matthews PM. Neocortical neuronal, synaptic, and glial loss in multiple sclerosis. *Neurology* 2006; **67**: 960–7
23 Klaver R, Popescu V, Voorn P, Galis-de Graaf Y, van der Valk P, de Vries H, Schenk GJ, Geurts JJ. Neuronal and axonal loss in normal-appearing gray matter and subpial lesions in multiple sclerosis. *J Neuropathol Exp Neurol* 2015; **74**: 453–8.
24 Filippi M, Evangelou N, Kangarlu A, Inglese M, Mainero C, Horsfield MA, Rocca MA. Ultra-high-field MR imaging in multiple sclerosis. *J Neurol Neurosurg Psychiatry* 2014; **85**: 60–6
25 Abdel-Fahim R, Mistry N, Mougin O, Blazejewska A, Pitiot A, Retkute R, Gowland P, Evangelou N. Improved detection of focal cortical lesions using 7T magnetisation transfer imaging in patients with multiple sclerosis. *Mult Scler Relat Disord* 2014; **3**: 258–65
26 Schmierer K, Parkes HG, So PW, An SF, Brandner S, Ordidge RJ, Yousry TA, Miller DH. High field (9.4 Tesla) magnetic resonance imaging of cortical grey matter lesions in multiple sclerosis. *Brain* 2010a; **133** (Pt. 3): 858–67
27 Popescu V, Klaver R, Voorn P, Galis-de Graaf Y, Knol DL, Twisk J, Versteeg A, Schenk GJ, Van der Valk P, Barkhof F, De Vries HE, Vrenken H, Geurts J. What drives MRI-measured cortical atrophy in multiple sclerosis? *Mult Scler* 2015; **21**: 1280–90.
28 Kuhlmann T, Ludwin S, Prat A, Antel J, Bruck W, Lassmann H. An updated histological classification system for multiple sclerosis lesions. *Acta Neuropathol* 2017; **133**: 13–24. Epub 2016/12/19
29 Gundersen HJ, Jensen EB. The efficiency of systematic sampling in stereology and its prediction. *J Microsc* 1987; **147**(Pt. 3): 229–63
30 Gundersen HJ. Stereology of arbitrary particles. A review of unbiased number and size estimators and the presentation of some new ones, in memory of William R. Thompson. *J Microsc* 1986; **143**(Pt. 1): 3–45
31 West MJ, Slomianka L, Gundersen HJ. Unbiased stereological estimation of the total number of neurons in the subdivisions of the rat hippocampus using the optical fractionator. *Anatl Rec* 1991; **231**: 482–97
32 Fabricius K, Jacobsen JS, Pakkenberg B. Effect of age on neocortical brain cells in 90+ year old human females–a cell counting study. *Neurobiol Aging* 2013; **34**: 91–9
33 Korbo L, Pakkenberg B, Ladefoged O, Gundersen HJ, Arlien-Soborg P, Pakkenberg H. An efficient method for estimating the total number of neurons in rat brain cortex. *J Neurosci Methods* 1990; **31**: 93–100
34 Pakkenberg B, Gundersen HJ. Neocortical neuron number in humans: effect of sex and age. *J Comp Neurol* 1997; **384**: 312–20

35 Gundersen HJ. Estimators of the number of objects per area unbiased by edge effects. *Microsc Acta* 1978; **81**: 107–17
36 Pelvig DP, Pakkenberg H, Stark AK, Pakkenberg B. Neocortical glial cell numbers in human brains. *Neurobiol Aging* 2008; **29**: 1754–62
37 Artacho-Perula E, Arbizu J, Arroyo-Jimenez Mdel M, Marcos P, Martinez-Marcos A, Blaizot X, et al. Quantitative estimation of the primary auditory cortex in human brains. *Brain research* 2004; **1008**(1): 20–8. Epub 2004/04/15.
38 Vollmer T, Signorovitch J, Huynh L, Galebach P, Kelley C, DiBernardo A, Sasane R. The natural history of brain volume loss among patients with multiple sclerosis: a systematic literature review and meta-analysis. *J Neurol Sci* 2015; **357**: 8–18
39 Steenwijk MD, Daams M, Pouwels PJ, Balk LJ, Tewarie PK, Killestein J, Uitdehaag BM, Geurts JJ, Barkhof F, Vrenken H. What explains gray matter atrophy in long-standing multiple sclerosis? *Radiology* 2014; **272**: 832–42
40 Schmierer K, Wheeler-Kingshott CA, Tozer DJ, Boulby PA, Parkes HG, Yousry TA, Scaravilli F, Barker GJ, Tofts PS, Miller DH. Quantitative magnetic resonance of postmortem multiple sclerosis brain before and after fixation. *Magn Reson Med* 2008; **59**: 268–77
41 Schmierer K, Thavarajah JR, An SF, Brandner S, Miller DH, Tozer DJ. Effects of formalin fixation on magnetic resonance indices in multiple sclerosis cortical gray matter. *J Magn Reson Imaging* 2010b; **32**: 1054–60
42 Dam M. Shrinkage of the brain during histological procedures with fixation in formaldehyde solutions of different concentrations. *J Hirnforsch* 1979; **20**: 115–19
43 Roosendaal SD, Bendfeldt K, Vrenken H, Polman CH, Borgwardt S, Radue EW, Kappos L, Pelletier D, Hauser SL, Matthews PM, Barkhof F, Geurts JJ. Grey matter volume in a large cohort of MS patients: relation to MRI parameters and disability. *Mult Scler* 2011; **17**: 1098–106
44 Zivadinov R, Uher T, Hagemeier J, Vaneckova M, Ramasamy DP, Tyblova M, Bergsland N, Seidl Z, Dwyer MG, Krasensky J, Havrdova E, Horakova D. A serial 10-year follow-up study of brain atrophy and disability progression in RRMS patients. *Mult Scler* 2016; **22**: 1709–1718.
45 Charil A, Dagher A, Lerch JP, Zijdenbos AP, Worsley KJ, Evans AC. Focal cortical atrophy in multiple sclerosis: relation to lesion load and disability. *NeuroImage* 2007; **34**: 509–17
46 Sailer M, Fischl B, Salat D, Tempelmann C, Schonfeld MA, Busa E, Bodammer N, Heinze HJ, Dale A. Focal thinning of the cerebral cortex in multiple sclerosis. *Brain* 2003; **126**(Pt. 8): 1734–44
47 Calabrese M, Reynolds R, Magliozzi R, Castellaro M, Morra A, Scalfari A, Farina G, Romualdi C, Gajofatto A, Pitteri M, Benedetti MD, Monaco S. Regional distribution and evolution of gray matter damage in different populations of multiple sclerosis patients. *PLoS ONE* 2015a; **10**: e0135428
48 Tillema JM, Hulst HE, Rocca MA, Vrenken H, Steenwijk MD, Damjanovic D, Enzinger C, Ropele S, Tedeschi G, Gallo A, Ciccarelli O, Rovira A, Montalban X, de Stefano N, Stromillo ML, Filippi M, Barkhof F. Regional cortical thinning in multiple sclerosis and its relation with cognitive impairment: a multicenter study. *Mult Scler* 2015; **22**: 901–9
49 Ferguson B, Matyszak MK, Esiri MM, Perry VH. Axonal damage in acute multiple sclerosis lesions. *Brain* 1997; **120**(Pt. 3): 393–9
50 Trapp BD, Peterson J, Ransohoff RM, Rudick R, Mork S, Bo L. Axonal transection in the lesions of multiple sclerosis. *N Engl J Med* 1998; **338**: 278–85
51 Coleman MP, Perry VH. Axon pathology in neurological disease: a neglected therapeutic target. *Trends Neurosci* 2002; **25**: 532–7
52 Trapp BD, Ransohoff RM, Fisher E, Rudick RA. Neurodegeneration in multiple sclerosis: relationship to neurological disability. *Neuroscientist* 1999; **5**: 48–57
53 Andrews HE, Nichols PP, Bates D, Turnbull DM. Mitochondrial dysfunction plays a key role in progressive axonal loss in multiple sclerosis. *Med Hypotheses* 2005; **64**: 669–77
54 Levin MC, Lee S, Gardner LA, Shin Y, Douglas JN, Cooper C. Autoantibodies to non-myelin antigens as contributors to the pathogenesis of multiple sclerosis. *J Clin Cell Immunol* 2013; **4**: 2–19
55 Howell OW, Rundle JL, Garg A, Komada M, Brophy PJ, Reynolds R. Activated microglia mediate axoglial disruption that contributes to axonal injury in multiple sclerosis. *J Neuropathol Exp Neurol* 2010; **69**: 1017–33. Epub 2010/09/15
56 Pomeroy IM, Jordan EK, Frank JA, Matthews PM, Esiri MM. Focal and diffuse cortical degenerative changes in a marmoset model of multiple sclerosis. *Mult Scler* 2010; **16**: 537–48
57 Fischer MT, Sharma R, Lim JL, Haider L, Frischer JM, Drexhage J, Mahad D, Bradl M, van Horssen J, Lassmann H. NADPH oxidase expression in active multiple sclerosis lesions in relation to oxidative tissue damage and mitochondrial injury. *Brain* 2012; **135**(Pt. 3): 886–99
58 Calabrese M, Magliozzi R, Ciccarelli O, Geurts JJ, Reynolds R, Martin R. Exploring the origins of grey matter damage in multiple sclerosis. *Nat Rev Neurosci* 2015b; **16**: 147–58
59 Ruckh JM, Zhao JW, Shadrach JL, van Wijngaarden P, Rao TN, Wagers AJ, Franklin RJ. Rejuvenation of regeneration in the aging central nervous system. *Cell Stem Cell* 2012; **10**: 96–103
60 Goldschmidt T, Antel J, Konig FB, Bruck W, Kuhlmann T. Remyelination capacity of the MS brain decreases with disease chronicity. *Neurology* 2009; **72**: 1914–21

61 Leray E, Yaouanq J, Le Page E, Coustans M, Laplaud D, Oger J, Edan G. Evidence for a two-stage disability progression in multiple sclerosis. *Brain* 2010; **133**(Pt. 7): 1900–13
62 Scalfari A, Neuhaus A, Degenhardt A, Rice GP, Muraro PA, Daumer M, Ebers GC. The natural history of multiple sclerosis: a geographically based study 10: relapses and long-term disability. *Brain* 2010; **133**(Pt. 7): 1914–29
63 Trapp BD, Nave KA. Multiple sclerosis: an immune or neurodegenerative disorder? *Annu Rev Neurosci* 2008; **31**: 247–69
64 Petrova N, Carassiti D, Altmann DR, Baker D, Schmierer K. Axonal loss in the multiple sclerosis spinal cord revisited. *Brain Pathol* 2017. doi: 10.1111/bpa.12516. [Epub ahead of print]
65 DeLuca GC, Williams K, Evangelou N, Ebers GC, Esiri MM. The contribution of demyelination to axonal loss in multiple sclerosis. *Brain* 2006; **129**(Pt. 6): 1507–16
66 Henstridge CM, Pickett E, Spires-Jones TL. Synaptic pathology: a shared mechanism in neurological disease. *Ageing Res Rev* 2016; **28**: 72–84
67 Mandolesi G, Gentile A, Musella A, Fresegna D, De Vito F, Bullitta S, Sepman H, Marfia GA, Centonze D. Synaptopathy connects inflammation and neurodegeneration in multiple sclerosis. *Nat Rev Neurol* 2015; **11**: 711–24
68 Dutta R, Trapp BD. Mechanisms of neuronal dysfunction and degeneration in multiple sclerosis. *Prog Neurobiol* 2011; **93**: 1–12
69 Michailidou I, Willems JG, Kooi EJ, van Eden C, Gold SM, Geurts JJ, Baas F, Huitinga I, Ramaglia V. Complement C1q-C3-associated synaptic changes in multiple sclerosis hippocampus. *Ann Neurol* 2015; **77**: 1007–26
70 Jurgens T, Jafari M, Kreutzfeldt M, Bahn E, Bruck W, Kerschensteiner M, Merkler D. Reconstruction of single cortical projection neurons reveals primary spine loss in multiple sclerosis. *Brain* 2016; **139**(Pt. 1): 39–46
71 Watkins LM, Neal JW, Loveless S, Michailidou I, Ramaglia V, Rees MI, Reynolds R, Robertson NP, Morgan BP, Howell OW. Complement is activated in progressive multiple sclerosis cortical grey matter lesions. *J Neuroinflammation* 2016; **13**: 161
72 Albert M, Barrantes-Freer A, Lohrberg M, Antel JP, Prineas JW, Palkovits M, Wolff JR, Bruck W, Stadelmann C. Synaptic pathology in the cerebellar dentate nucleus in chronic multiple sclerosis. *Brain Pathol* 2016. doi: 10.1111/bpa.12450

Supporting information

Additional Supporting Information may be found in the online version of this article at the publisher's web-site:

Figure S1. Findings suggestive of additional neurodegenerative pathology. Positive tissue controls for α-synuclein (**A**), αβ-amyloid (**B**) and Tau (**C**). Images acquired with a 40× objective, scale bar = 30 μm. No Lewy bodies and/or synuclein-positive intracytoplasmatic inclusions were observed in any of the brains examined: controls (**D**) and multiple sclerosis (MS) (**G**), images acquired with 20× objective, scale bar = 100 μm. Sparse αβ-amyloid plaques were observed in the neocortex, but not the hippocampus, of one control (**E**, image acquired with a 20× objective, scale bar = 100 μm) and one people with MS (**H**, image acquired with 10× objective, scale bar = 100 μm). Very sparse Tau-positive neurons were observed in the dentate gyrus and the neocortex of one healthy control (**F**) and two MS cases (**I**), images acquired with a 20× objective, scale bar = 100 μm.
Table S1. All antibodies and antigen retrieval details.

Received 22 December 2016
Accepted after revision 11 April 2017
Published online Article Accepted on 18 April 2017